Bioinspired synthesis and characterization of gold nano-particles from medicinally important *Periploca hydaspidis* and their *in vitro* antioxidant and antimicrobial activity

Rafi Ullah[1], Jehan Bakht[1]*, Muhammad Raza Shah[2] and Mohammad Shafi[3]
[1]Institute of Biotechnology and Genetic Engineering, The University of Agriculture Peshawar, KPK, Pakistan
[2]International Center for Chemical and Biological Sciences, HEJ Research Institute of Chemistry, University of Karachi
[3]Department of Agronomy, The University of Agriculture, Peshawar, KPK, Pakistan

Abstract: This research investigates the synthesis and characterization of gold nanoparticles from *Periploca hydaspidis* and their antimicrobial and anti oxidant activity. The synthesis of AuNPs was confirmed by UV-Vis spectrophotometer and structure by a high resolution atomic force microscope. X-ray diffraction and Fourier transformed infrared spectroscopy was used to study the crystallite size and different functional groups. DPPH radical scavenging activity and disc diffusion protocol was applied for the determination of antioxidant and antimicrobial activity. A ratio of 1:8 of 1mM $AuCl_3$ solutions with plant boiled extract used for synthesis of gold nano-particles. The formation of the gold nano-particles was determined by the color change from yellow to dark purple which were confirmed by UV-Vis spectrophotometer. Gold nano-particles were stable between 24°C and 39°C, mM concentration of the salt and neutral pH. The groups responsible for the synthesis of gold nano-paricles were Alkenes and aliphatic amines. The AuNP were cubic in nature and the nanocrystallite size was 6.99nm. Gold nano-particles revealed good antioxidant activity and controlled the growth of *K. pnemoniae, E. coli, X. compestris, C. albicans* and *P. chrysogenum*.

Keywords: Nano-particles, AuNPs, AFM, FT-IR, XRD, *Periploca hyaspidis,* disc diffusion.

INTRODUCTION

Nano-particles synthesis and their characterization are of vital importance due to their wider application in different areas research area of physical and natural sciences including physics, chemistry medicine and biology (Song and Kim, 2009). In recent times the synthesis of mono-dispersed nano-particles with different sizes and shapes has been a challenge. Metal nano-particles are particularly interesting at nano-scale system because of the ease in its synthesis and chemical modifications. Optoelectronic, physicochemical and electronic properties of metal nano-particles are determined by their size, shape and crystalline nature. Different methods including physical, chemical and biological are used to synthesize metal nano-particles. In chemical methods hazardous substances such as sodium borohydride, tetrakish-hydroxymethyl-phosphonium chloride (THPC), poly-N-vinyl pyrrolidone (PVP) and hydroxylamine have been used for the synthesis of nano-particles. Toxic chemicals on the surface of nano-particles and non-polar solvents in the synthesis limit their applications in clinical fields. Therefore, biological methods including both extra and intra-cellular synthesis of nano-particles are preferred for the production of clean, biocompatible, non toxic and environment friendly. Recently living cells have been used to synthesize nano-particles. Silver nano-particles were synthesized extra-cellular by the fungus *Aspergillus fumigates* (Mann, 1996). Gold nano-particles can also be produced by other fungi and a number of bacterial species (Phillip *et al*., 2006). Besides microorganisms like bacteria and fungi, plants can also be used for the production of nano-particles. The use of plants in the synthesis of nano-particles has turn out to be one of the accepted alternatives for traditional chemical and physical methods. Several plants including *Pelargonium graveolens*, *Cymbopogon flexuosus* and *Aloe vera* etc. have been used for the production of nano-particles (Shankar *et al*., 2003; Chandran *et al*., 2006).

Characterization is necessary for the control and applications of nano-particles. A wide range of special techniques including ultraviolet-visible spectroscopy, atomic force microscopy (AFM), electron microscopy (TEM, SEM), powder x-ray diffraction (XRD), x-ray photoelectron spectroscopy (XPS), dynamic light scattering (DLS), matrix-assisted laser desorption/ionization time-of-flight mass spectrometry (MALDI-TOF), fourier transform infrared spectroscopy (FT-IR) and nuclear magnetic resonance (NMR) are used for the characterization of nano-particles. These techniques used for the characterization of nano-particles are light-based, however, a non-optical nano-particles characterization technique (Tunable Resistive Pulse Sensing (TR-PS) is also in for the measurement of size, surface charge and concentration of nano-particles (Prime and Whitesides, 1991). The aims of the present study were (1) bioinspired synthesis and characterization of

Corresponding author: e-mail: jehanbakht@yahoo.co.uk

Table 1: Bacterial strains used during the present study and their origin

Microbial Species	Gram stain type	Details
Klebsiella pneumonia	Negative	Clinical isolate, Quaid-E-Azam University Islamabad Pakistan.
Pseudomonas aeruginosa	Negative	ATCC # 9721
Staphylococcus aureus	Positive	ATCC # 6538
Bacillus subtilis	Positive	Clinical isolate, Quaid-E-Azam University Islamabad Pakistan.
Escherichia coli	Negative	ATCC # 25922
Xanthomonas campestris	Negative	ATCC # 33913
Citorbacter freundii	Negative	ATCC # 8090

Table 2: Fungal strains used during the present study and their origin

Name of the specie	Details of the specie used
Candida albicans	ATCC #10231 Plant Pathology Department The University of Agriculture Peshawar, Pakistan
Trichoderma reesei	ATCC #26921 Plant Pathology Department The University of Agriculture Peshawar, Pakistan
Acremonium alternatum	ATCC #60645 Plant Pathology Department The University of Agriculture Peshawar, Pakistan
Penicillium chrysogenum	ATCC #11709 Plant Pathology Department The University of Agriculture Peshawar, Pakistan
Rhizopus oryzae	ATCC # 20344Plant Pathology Department The University of Agriculture Peshawar, Pakistan

gold nano-particles from *Periploca hydaspidis* and (2) to investigate anti-bacterial, anti-fungal and antioxidant activities of gold nano-particles from *Periploca hydaspidis*.

MATERIALS AND METHODS

Collection and identification of plant material

Plants of *Periploca hyaspidis* was collected from different areas of Madyan and Marghuzar of Swat valley of Khyber Pukhtun Khwa (KPK) province of Pakistan. The plant specimen was identified by plant taxonomist at the Department of Botany, government post-graduate Jehan Zeb College Swat (KPK).

Table 3: Showing possible formulated structures of AuNPs and one by one fragmentation of the gold molecules from $AuCl_3$

Charged fragments	Possible structure $[Au_xL_xCl_y]^{x+}$
3740.82	$Au_{17}L_xCly$
3544.84	$Au_{16}L_xCly$
3347.84	$Au_{15}L_xCly$
3150.84	$Au_{14}L_xCly$
2953.87	$Au_{13}L_xCly$
2756.87	$Au_{12}L_xCly$
2559.92	$Au_{11}L_xCly$
2362.96	$Au_{10}L_xCly$
2167.34	$Au_{09}L_xCly$
1969.98	$Au_{08}L_xCly$
1773.00	$Au_{07}L_xCly$
1576.01	$Au_{06}L_xCly$
1379.01	$Au_{05}L_xCly$
1174.11	$Au_{04}L_xCly$
985.02	$Au_{03}L_xCly$
780.10	$Au_{02}L_xCly$
575.17	$Au_{01}L_xCly$

Preparation of plant extract

Aqua-regia and de-ionized water was used to wash all the glass wares used for the synthesis of AuNPs. Twenty grams of dried grinded material of *Periploca hydaspidis* plant was soaked in 50ml of de-ionized water for 24 hours, boiled to get the extract and then filtered through Whatman No. 1 filter paper. The filtrate was used for the synthesis of nano-particles.

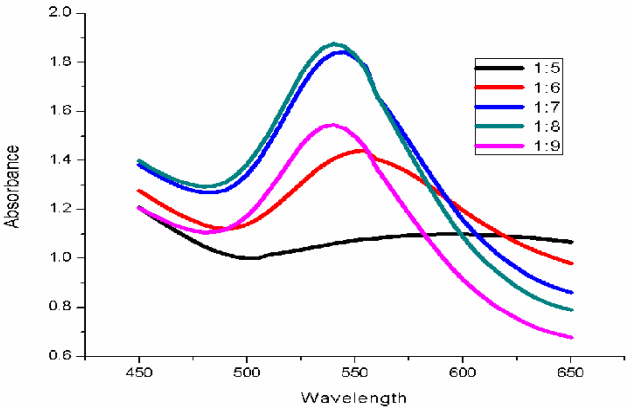

Fig. 1: Comparison of different UV-Vis spectrums of AuNPs produced by combination of the boiled plant extract (1ml) with different ratios of $AuCl_3$ (1mM) solution.

Synthesis of the nano-particles

One mM $AuCl_3$ solution was prepared and stored in amber color bottle. Fifteen test tubes were added with 1ml of the plant extract. To these test tubes, 1mM $AuCl_3$ solution was added drop wise with constant stirring at the ratio of 1:1, 1:2 up to 1:15 and incubated at for 48 hours (room temperature). The color change of the extract from yellow to brown revealed the synthesis of gold nano-particles.

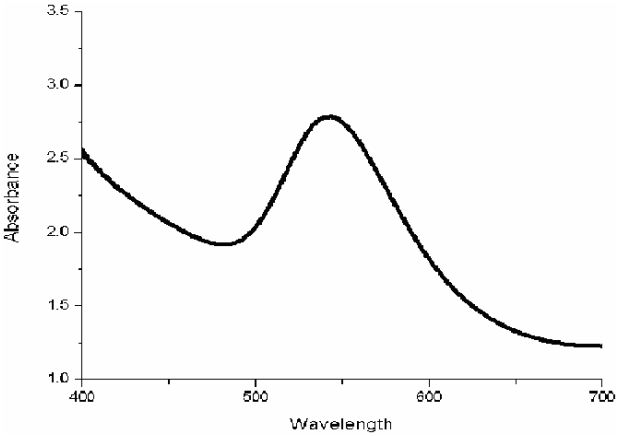

Fig. 2: UV-Vis spectrum of AuNPs produced by combination of 1ml boiled plant extract with 8ml of $AuCl_3$ (1mM) solution showing the peak of the AuNPs at 544nm.

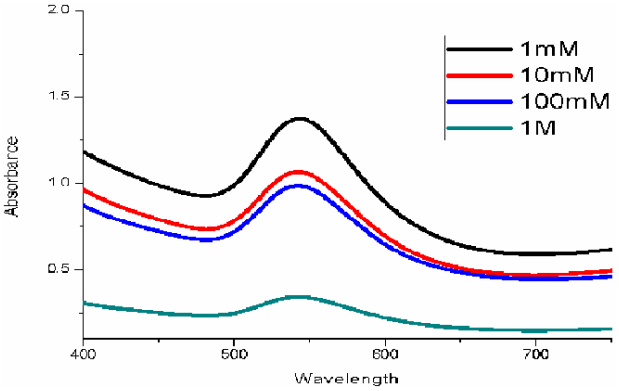

Fig. 3: Comparison of UV-Vis spectrums of AuNPs isolated at different temperatures.

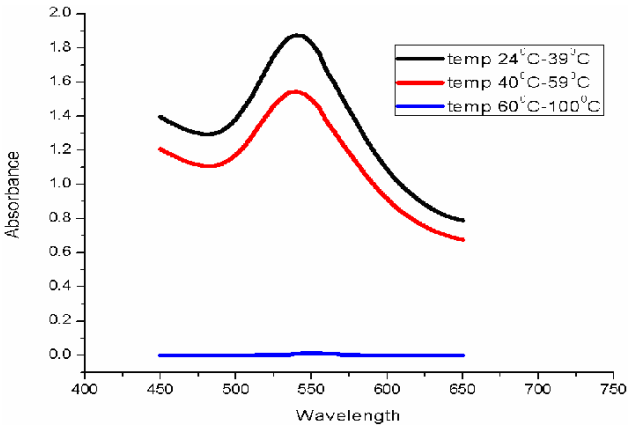

Fig. 4: Comparison of UV-Vis spectrums of AuNPs treated with different salt (NaCl) concentrations.

Characterization of the synthesized gold nano-particles

UV-visible spectrophotometer study

The reduction of pure gold ions to AuNPs was monitored by UV-Vis spectrometer. The AuNPs solutions were diluted with de-ionized water at the ratio of 1:2. The UV-Vis spectral analysis was carried out using UV-Vis spectrophotometer (UV Probe, version 2.42 of Shimadzu, Japan) (Ateeq *et al*., 2015).

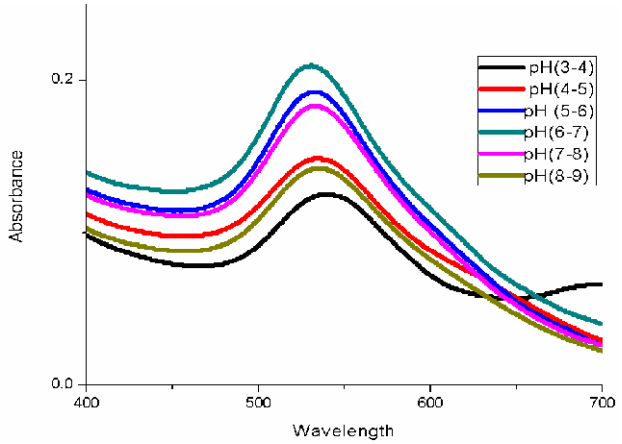

Fig. 5: Comparison of UV-Vis spectrum of AuNPs treated with different pH stress levels ranging from 3 to 9.

Atomic force microscopic analysis

Topographic images were taken using a high resolution atomic force microscope (Agilent-5500 AFM, operated in tapping mode to determine the structure of the synthesized AuNPs from *Periploca hydaspidis* plant extract. Sample was prepared by adsorption of NPs on the surface of mica and was allowed to evaporate at ambient conditions for imaging as described by Ateeq *et al*. (2015).

X-ray diffraction (XRD) analysis

Snidjer Freeze dryer (Snidjers Scientific Model LYSFME Holland) was used to freeze the synthesized AuNPs. For random distribution, a few grams of freeze dried NPs were smeared uniformly onto a glass slide, assuring a flat upper surface. X-ray diffracto-meter equipped with target source of Cu having tube voltage of 40kV, 1 degree divergence slit, 2 degree scattering slit, 0.2mm receiving slit and 2theta ordinary mode with 2sec count time by step method was used to determine the particle sizes and crystallite nature of the NPs. Origin pro 8 software. The crystallite size for the AuNPs was calculated was used to analyze the recorded data using Sherrer's equation.

$$Dp = 0.94\lambda/\beta_{1/2}\cos\theta$$

Where Dp is average crystallite size, λ is X-ray wavelength, β represents line broadening in radians and θ is Bragg's reflection angle (Valentina and Minaev, 2014).

Fourier transformed infrared (FT-IR) spectroscopy

FT-IR spectrophotometer (Shimdzu IR 460) was used for FT-IR analysis. The plant extract and the sample containing AuNPs were freeze dried separately and analyzed through FT-IR. Different modes of vibrations were identified to investigate different functional groups present in AuNPs (Dubey *et al*., 2013).

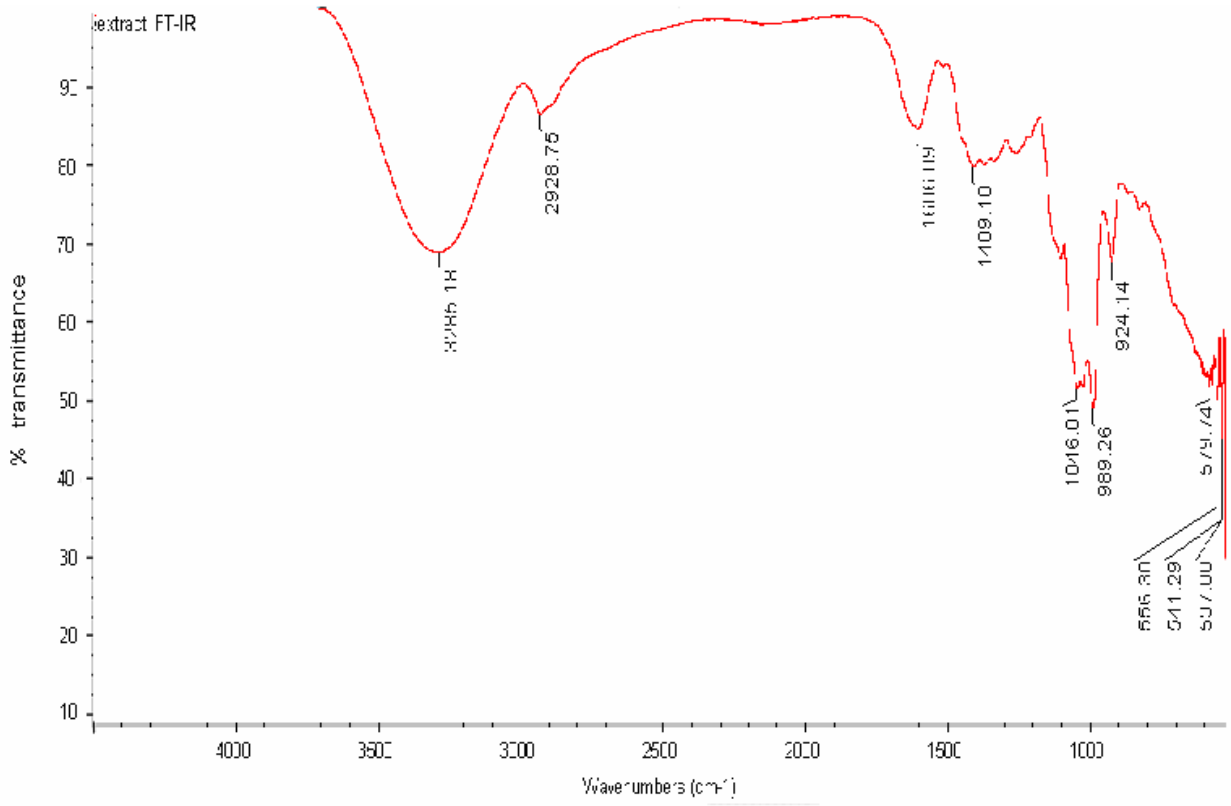

Fig. 6: FT-IR spectra of the pure boiled plant extract, showing absorption bands with percent transmittance at different wave numbers cm^{-1}.

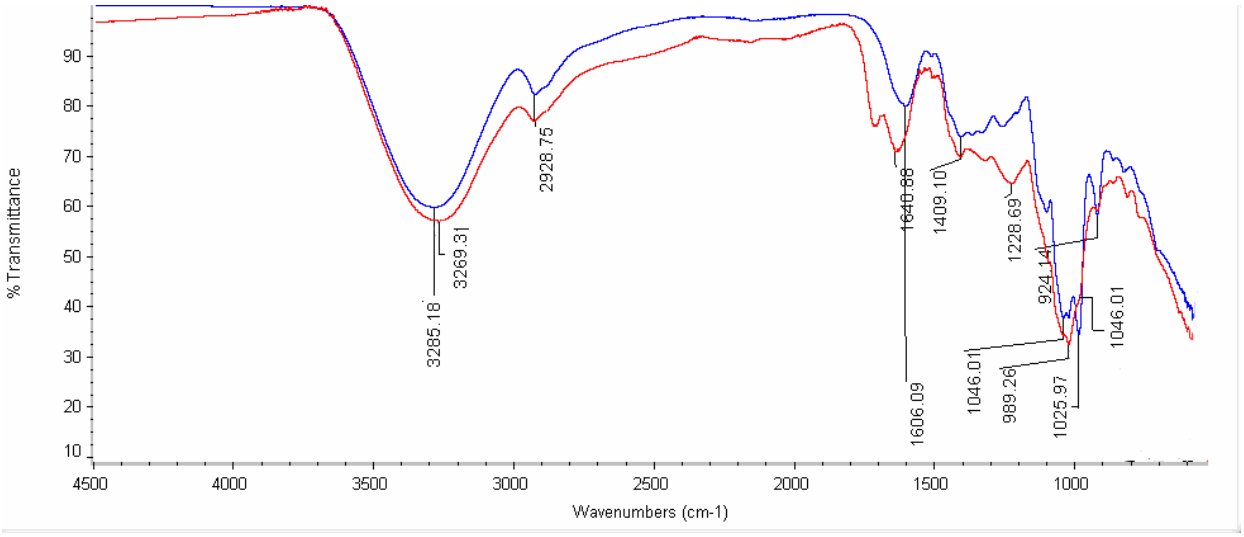

Fig. 7: Comparative FT-IR spectra of boiled plant extract and AuNPs, showing absorption bands with percent transmittance at different wave numbers cm^{-1}.

Antimicrobial activity

Disc diffusion assay as described by Bauer *et al*. (1966) was used to carry out the antibacterial activity of the synthesized nano-particles from *Periploca hydaspidis* against different bacterial strains. Nutrient agar media plates were inoculated with 18-24hrs cultures of microbial inoculums. Three separate discs of Whatman No. 1 filter paper (6mm in diameter) were placed on the media in petri plates. Gold nano-particles in concentrations of 300, 400 and 500ppm ml^{-1} were applied on the discs and kept at 37ºC for 18-24hrs. Zones of inhibition were recorded in mm around the discs in each plate next day. The experiments were carry out in triplicate and the zone of inhibitions was determined by the following formula.

$$\text{Inhibition \%} = \frac{\text{Zone of sample}}{\text{Zone of control}} \times 100$$

Antifungal potential of the gold NPs were tested against fungal strains shown in table 2 (Ramadas *et al*., 1998). Commercially available Potato Dextrose Agar (PDA) media was used to culture different fungal strains and sub cultured on potato dextrose agar (PDA) media containing 104 cells ml^{-1}. AuNPs in concentration of 300, 400 and 500 ppm were applied onto the disc. The zone of inhibition was measured in mm after seventh day of the culturing. The experiments were conducted three times and the zone of inhibitions was calculated using the following formula.

$$\text{Inhibition \%} = \frac{\text{Zone of sample}}{\text{Zone of control}} \times 100$$

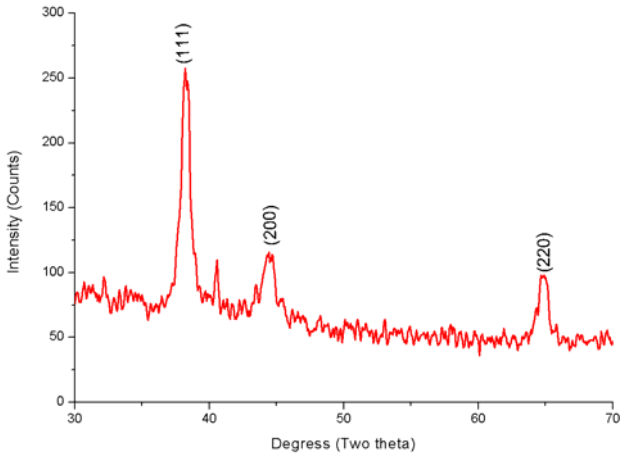

Fig. 8: XRD patterns of AuNPs showing the intense reflections with 2θ valves. Matrix Assisted Laser desorption/ionization-Time of Flight (MALDI-TOF) Mass Spectroscopy analysis of AuNPs

Positive control

Ciprofloxacin (50µg/6µl) was used as positive control against gram positive and gram negative bacteria and Fluconazole at the same concentration as positive control for fungi. In both the cases DMSO was used as negative control.

The culture media

Nutrient Broth Modified media QUE-LABQB-39-3504 was used for the standardization and shaking incubation of microbes and Nutrient Agar Modified media QUE-LABQB-39-3504 for culturing and growth of the microbes, (Bakht *et al.,* 2017; Wajid *et al*., 2017).

DPPH radical scavenging activity

The method described by Mensor *et al*. (2001) was used to study DPPH radical scavenging activity of AuNPs. The stock solutions of the samples were diluted to final concentrations of 250, 125, 50, 25, 10 and 5µg ml^{-1} in methanol. One ml of a 0.3mM DPPH methanol solution was mixed with 2.5ml solution of the extract and allowed to react for 30min at room temperature under complete dark. The absorbance of the resulting mixture was measured at 518nm using UV visible spectrophotometer. The readings were converted to percentage antioxidant activity (% AA) by the following formula

$Q= 100(A_o-A_s)/A_o$

Where; Q = % antioxidant activity, A_o =Absorbance of Pure DPPH and A_s = Absorbance of the sample.

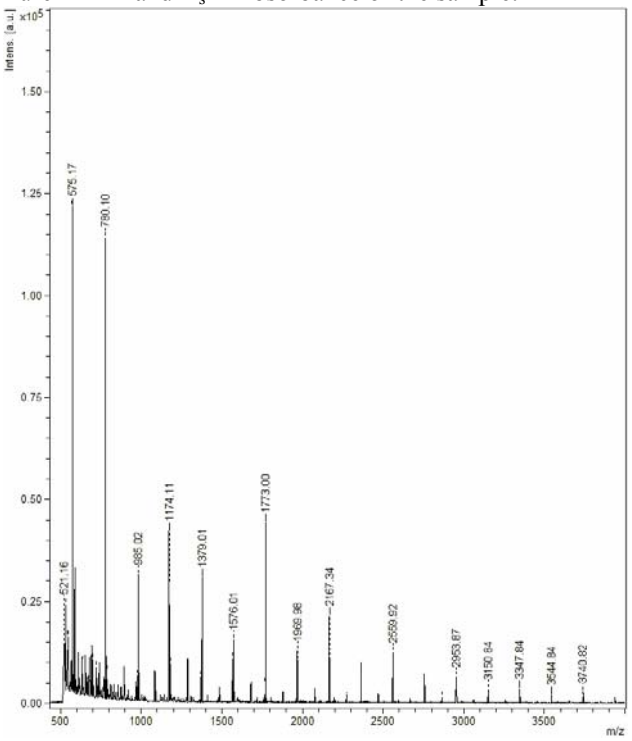

Fig. 9: MALDI-TOF spectrum indicating the fragmentation patterns of gold molecules in AuNPs. m/z represents the mass to charge ratio at x-axis while Y-axis represents the intensity of gold molecules.

STATISTICAL ANALYSIS

For statistical analysis, MSTATC computer software was used (Russel and Eisensmith, 1983). Least Significant Difference (LSD) test was used to separate differences among means (Steel *et al*., 1997). Data are presented as mean values of three replications.

RESULTS

Synthesis and confirmation of gold nano-particles (AuNPs)

The synthesis of AuNPs was monitored and confirmed both visually and using UV-Vis spectro-photometer. The synthesis of the AuNPs was observed visually with naked eyes. After the addition of $AuCl_3$ solution to the plant extract, the color of the extract turned from yellow to dark purple which confirmed the formation of AuNPs. The data revealed that as the ratio of plant extract to $AuCl_3$ increased, the color of the solution got dense due to the formation of large amount of nano-particles. The

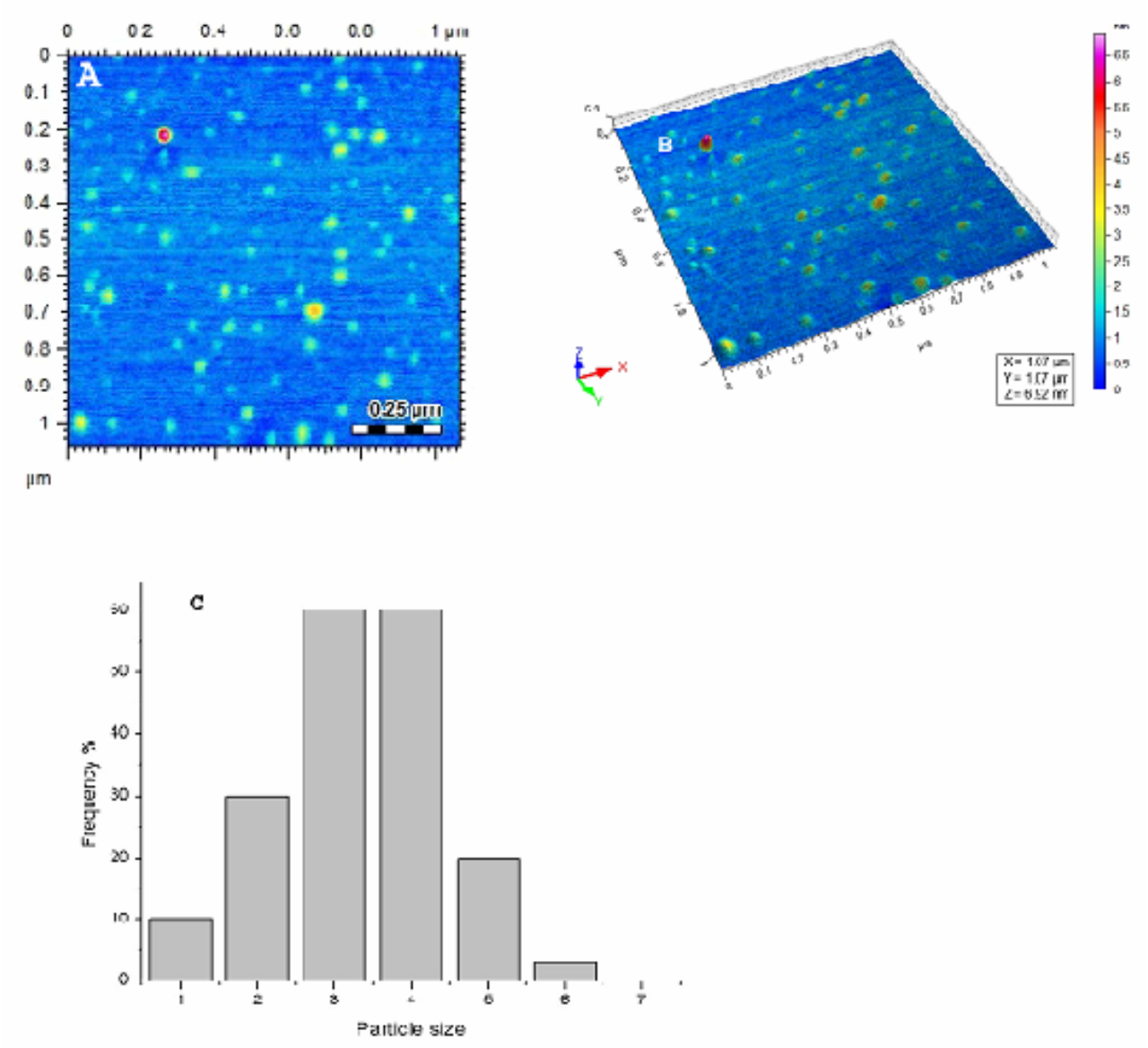

Fig. 10: AFM investigation of AuNPs (a) Topography (b) Two dimensional view of nano-particles (c) Particle size distribution

appearance of purple color represented the formation of very small nano-particles. UV-Vis spectrum of the AuNPs synthesized by different combination of the boiled plant extract and 1mM of $AuCl_3$ solution is presented fig. 1. The spectrum indicated that the highest peak was given by mixing of 1ml of boiled plant extract with 8ml of $AuCl_3$ solution (1:8), while the smallest peak by combining 1ml of the plant extract and 5ml of $AuCl_3$ solution (1:5). At lower ratios no detectable nano-particles were produced. As the highest peak was given at 1:8, therefore, this ratio of plant extract and $AuCl_3$ was used for further studies. The synthesis of AuNPs from 1mM solution of $AuCl_3$ (1:8 ratios) was further confirmed using UV-Vis Spectrophotometer analysis of the samples. fig. 2 revealed the spectrum of the sample taken after 24 hours of the preparation. The spectrum indicated that the highest absorption point of the peak was 2.788 at 544nm, which lies in the region for the absorbance of AuNPs (500nm-600nm).

Stability study of AuNPs

Effect of temperature, salt and pH on AuNPs

The data revealed that the stability of AuNPs decreased with increasing temperature. The AuNPs were more stable between 24°C and 39°C as indicated by the highest peak of the spectrum (fig. 3). The fig. also showed that with increasing temperature, stability of AuNPs was decreased as indicated by the spectrum of the samples isolated between 40°C and 59°C. The peak of the samples at this temperature was lower than the peak from 24°C to

39°C resulting in the destabilization of the nano-particles with elevated temperatures. The samples isolated at 69°C to 100°C revealed that majority of the nano-particles were destroyed at these temperatures as indicated by no absorbance. The blue line in the graph represents the absorption at 69°C to 100°C. The effect of salt stress on AuNPs is shown in fig. 4. The UV-Vis spectrum of the salt stress samples indicated that AuNPs were more stable at mM than molar concentrations. The fig. also revealed that AuNPs were most stable at 1mM concentration and the stability decreased when the concentration of the salt increased. At 10 and 100mM salt stresses, the AuNPs were less stable compared to 1mM. The data recorded from the AuNPs treated with 1M salt revealed that the nano-particles were least stable at this concentration of salt and almost all the synthesized nano-particles were destroyed. The effect of pH on the stability and formation of AuNPs was also investigated through UV-Vis Spectrophotometer. The acidic pH stress was imposed by 1N HCl solution while basic pH stresses by 1N NaOH solution. The AuNPs formed were subjected to a broader range of pH of 3 to 9 (fig. 5). The AuNPs were found to be more stable at mildly acidic to neutral pH as the highest peak was given at pH range from 6 to 7, facilitating the nucleation of the nano-particles. The AuNPs were quite stable at pH 7-8 (mildly basic) and pH 5-6 (mildly acidic), however, were very less stable at highly basic pH of 8-9 and highly acidic pH of 3-4, adversely affecting nucleation process.

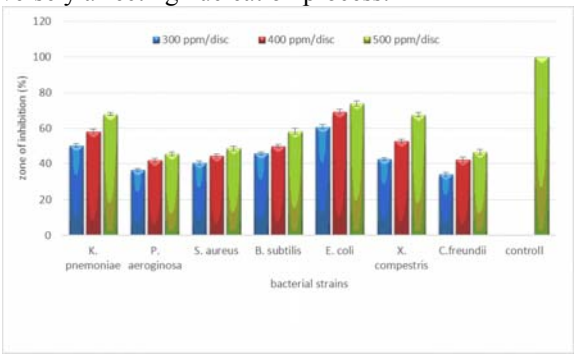

Fig. 11: Antibacterial activity of AuNPs against different bacterial strains by disc diffusion assay (Bar shows LSD at P<0.05).

Comparative FT-IR analysis of pure plant boiled extract and AuNPs

The spectra of Fourier Transformed Infrared (FTIR) spectroscopic analysis of the plant pure extract is shown in fig. 6. The spectra indicated that the plant pure extract sample showed absorptions bands at wave numbers 3285.18, 2928.75, 1606.09, 1409.10, 1046.01, 989.26, 924.14 and 579.74cm^{-1}. The broader stretch at 3285.18 cm^{-1} and 2928.75cm^{-1} was the confirmation of -O-H functional group representing the presence of alcohol and/or free water. The absorption band at 1046.01 cm^{-1} shows the -C-N functional group of aromatic amines, 989.26cm^{-1} showed the functional groups, =C-H, of alkenes, 924.14cm^{-1} confirms the presence of - [C=O-O-H] which is the functional group of carboxylic acid and 579.74cm^{-1} indicated the -N-H bend of Amines in this FT-IR spectra of the boiled plant extract.

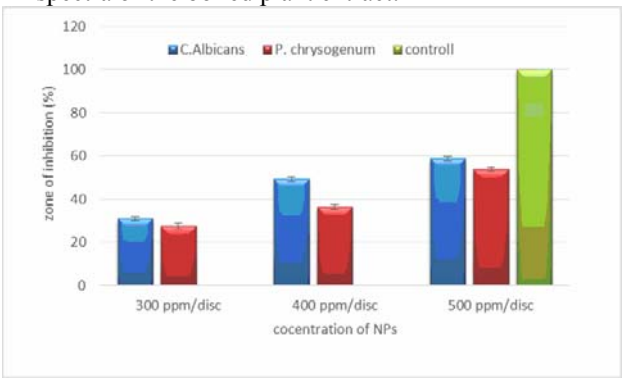

Fig. 12: Antifungal activity, of AuNPs against *C. albicans* and *P. chrysogenum* (Bar shows LSD at P<0.05).

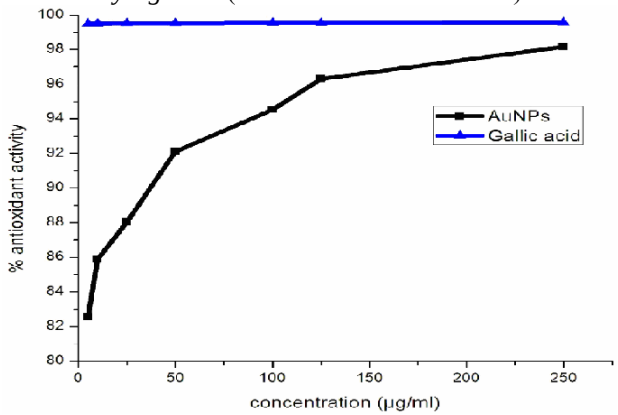

Fig. 13: Antioxidant activity of AuNPs using gallic acid as a standard

The spectra of Fourier Transformed Infrared (FT-IR) spectroscopic analysis of the plant extract treated with $AuCl_3$ containing AuNPs is shown in fig. 7. The comparison of the FT-IR spectra of AuNPs and pure plant boiled extract indicated that the absorption bands at 989.26 cm^{-1} and 1228.69cm^{-1} disappeared completely which shows alkenes and aliphatic amines respectively. The disappearance of these two peaks indicated that the =C-H and -C-N, functional group containing compounds played a role in the reduction of Au^{++} of $AuCl_3$ to AuNPs. The results of the FT-IR spectrum of pure plant boiled extract and the synthesized AuNPs further showed that there was a minute change from ±1 to ±100 wave numbers in other absorptions bands. The comparison of the two spectra indicated the shift of the wave numbers at the larger stretch of 3285.18cm^{-1} to 3269.31cm^{-1}, 2928.75 cm^{-1} to 2905.75cm^{-1}, 1606.09cm^{-1} to 1640.80cm^{-1},1409.10 cm^{-1} to 1228.69cm^{-1} and 1046.01cm^{-1} to 1025.97cm^{-1} can also be seen.

X-Ray Diffraction (XRD) analysis of AuNPs

The two theta (2θ) valves of a number of Bragg's reflections were 38.03°, 46.18° and 63.43° which

corresponds to (111), (200) and (220) facets of AuNPs which may be demonstrated as the bands for face centered cubic structures of Au (fig. 8). The XRD pattern of the freeze dried samples of AuNPs showed that synthesized AuNPs were 6.99nm in size and crystalline in nature which agree with the AFM data. The sharpness of the first peak revealed that the synthesized AuNPs were in nano region. The data also indicated that there were no peaks for the XRD patterns and the synthesized AuNPs were highly in pure form.

For the confirmation of possible structure of AuNPs, MALDI-TOF mass spectrophotometry was carried out (table 3 and fig. 9). The data in table 3 indicated that one gold molecule was lost during fragmentation (atomic weight of Au is 196.97amu and Cl is 35.5amu). The difference among all the peaks was almost 197 indicating that only one gold molecule was fragmented during the process. The extract can contain a large number of molecules, and the moment of fragmentation of the molecule could not be determined. Therefore, the contribution from the extract is designated as 'L_x', the contribution from the Chloride is designated as 'Cl_y' and the gold atom which is lost during fragmentation is shown as Au_x, thus the possible formulated structure was $[Au_xL_xCl_y]^{x+}$. It can be deduced from the spectrogram that the fragmentation of Au and extract was in 1:1 ratio where $AuCl_3$ lose one gold atom during fragmentation and the ligand was intact.

Determination of gold nano-particles size by atomic force microscope (AFM)

AFM was used to determine the particle size and its morphology (fig. 10). The data showed different sizes of the prepared particles. The smallest nano-particle was found to be 1.5nm in diameter while the largest was 6.5nm. The data in fig. 10 also showed that 60% of the particles synthesized were in the range of 3-4nm, 10% in 1-2nm, 30% in 2-3nm, 20% in 5-6nm while 4% of the AuNPs were synthesized in the range of 6-7nm.

Antimicrobial activity of AuNPs

Fig. 11 shows the antibacterial activity of AuNPs. Maximum zone of inhibition was shown by AuNPs at 500ppm against *E. coli* (73.81% ZI) while minimum was demonstrated at 300ppm against *P. aeruginosa* and *C. freundii* (33.91% ZI). *K. pnemoniae, E. coli* and *X. compestris* measured highest degree of sensitivity to AuNPs, *B. subtilis* and *C. freundii* showed moderate sensitivity while *P. aeroginosa*, *S. aureus* and *C. freundii* exhibited least sensitivity. The antibacterial activity was dose dependent and increasing concentration of the nano-particles increased its activity.

The antifungal activity of AuNPs of *Periploca hydaspidis* against *C. albicans* and *P. chrysogynum* is presented in fig. 12. The data suggested that *C. albicans* was responsive to AuNPs at all concentrations used. Maximum growth inhibition was demonstrated by AuNPs at 500ppm (58.78% ZI) followed by 49.27% ZI at 400 ppm. Minimum growth retardation (31.03% ZI) was achieved at 300 ppm. The data also revealed that *P. chrysogynum* was sensitive to AuNPs at all the tested concentrations. Maximum zone of inhibition (53.83% ZI) was demonstrated by AuNPs at 500ppm followed 400 ppm (36.57%). The data further indicated that lowest zone of inhibition of 27.60% ZI was measured at 300 ppm. All the other strains used during the present study were completely resistant to AuNPs at all concentrations used (Data not shown).

Antioxidant activity of AuNPs

The antioxidant potential of AuNPs is shown in fig. 13. The data revealed that AuNPs revealed maximum antioxidant potential of 98.16% at 250 µg/ml followed by 85.09% (AuNPs) at 5 µg/ml. The data indicated that AuNPs exhibited better scavenging activity compared with positive control (gallic acid).

DISCUSSION

The green synthesis of gold nano-particles (AuNPs) from 1mM solution of $AuCl_3$ was monitored and confirmed visually through UV-Vis Spectrophotometer. The color of the extract changed from yellow to dark purple by the addition of $AuCl_3$ solution to the plant extract which confirmed the synthesis of AuNPs. The change in color was due to the reduction of different bioactive molecules present in the extract responsible for the formation of the nano-particles (Ashok *et al*., 2010). AuNPs possesses free electrons which give rise to Surface Plasmon Rasonance (SPR) (Kumar *et al*., 2011). The vibration of the electrons of AuNPs with the light wave produces a resonance which was measured by the detector of the UV-Vis Spectrophotometer (Ravindran *et al*., 2010). During the present experiment, for the synthesis of larger amount of nano-particles, different combinations of the boiled plant extract and 1mM of $AuCl_3$ solution was used. Analysis of the data indicated that combination of 1ml of boiled plant extract and 8 ml of $AuCl_3$ solution (1:8) produced highest peak observed through UV-Vis spectroscopy for AuNPs. The smallest peak was given by mixing of plant extract and $AuCl_3$ solution in the ratio of 1:5. Further increase in the amount of the $AuCl_3$ produced blue shift indicating the instability and destruction of the nano-particles. This may be due the less availability of the Au ions or the total engagement of the compounds responsible for the synthesis of the AuNPs (Amarendra and Gopal, 2010). Spectrophotometer analysis revealed that the highest absorption point at SPR peak was noted at 544nm which were in the region for absorbance of AuNPs (500nm-600nm) (Ocanas *et al*., 2010).

The AuNPs synthesized were also checked for its stability against different parameters like temperature, pH and different salt concentrations (Malarkodi *et al*., 2013). The

samples isolated at different temperatures revealed that the stability of AuNPs decreased with increasing temperature which may be due to the destruction of the active components loaded onto the metal particles (Paulkumar *et al*., 2013). Gold nano-particles were most stable in the temperature range from 24°C to 39°C measuring the highest peak. Stability of AuNPs decreased as the temperature increased from 40°C to 59°C. The peak of the samples isolated at this temperature was lower than the peak of the samples isolated at 24°C to 39°C. AuNPs isolated at 69°C to 100°C showed that NPs were destroyed as almost no absorbance was recorded (Paulkumar *et al*., 2013).

AuNPs were more stable at salt stress given at mM than molar concentrations. The same results were also demonstrated by Gnanajobitha *et al*. (2013). Stability of AuNPs decreased as the concentration of the salt increased. The data recorded from the AuNPs treated with 1M salt revealed that the NPs were least stable at this concentration of salt. All these observations are in agreement with Noruzi *et al*. (2011).

The UV-Vis spectrogram demonstrated that the AuNPs synthesized were subjected to different pH ranges from 3 to 9. It was noticed that pH play a significant role in the synthesis and stability of AuNPs. It is reported that pH control the shape, size and crystalline nature of the AuNPs (Raghavan *et al*., 2014). Our results demonstrated that at lower acidic pH, large sized AuNPs were synthesized while at higher alkaline/basic pH, the size of AuNPs were small. Similar results are also reported by Lim *et al*. (2013). The AuNPs were found to be more stable at mildly acidic to neutral pH as the highest peak was given at pH of 6-7. The studies of Huang *et al*. (2007) revealed that pH had a profound effect on the size, shape and hence on the stability of the AuNPs. They concluded that the aggregation of AuNPs had likely to outclass the nucleation process at lower acidic pH. The blue shift in the spectrogram revealed the synthesis of AuNPs having small diameter. Ravichandran *et al*. (2011) reported that lower acidic pH decreased the synthesis of AuNPs and vice versa. These results clearly confirm our findings as our studies showed that the formation and stability of gold nano-particles are adversely affected both at higher acidic and higher alkaline pH, while stable particles were produced at neutral pH. At basic and acidic pH, nano-particles formed aggregation which may be responsible for its disintegration, while at mildly acidic to neutral pH no aggregation of AuNPs occurred, measuring sharp and highest peak. Generally, the AuNPs showed more stability at mildly acidic and mildly basic pH. The AuNPs were quite stable at pH 7-8 (mild basic) and at pH 5-6 (mild acidic). It was noted that at highly acidic or highly basic pH no synthesis of AuNPs occurred, which possibly will be due to the fact that higher positive charge at the surface of AuNPs attracted the negatively charged biomass resulting in flocculation (Krishnaraj *et al*., 2012).

The interaction of a photon of a specific wavelength with molecules stimulates a specific vibration mode. This stimulation of vibration mode causes an increase in the intensity of vibration which in turn causes constructive interference giving a peak at the end. This constructive interference leads to the identification of different functional groups present in the extract by giving specific spectra (Genc *et al*., 2011). The spectra of fourier transformed infrared (FTIR) spectroscopic analysis of the plant pure extract revealed absorptions bands at wave numbers 3285.18, 2928.75, 1606.09, 1409.10, 1046.01, 989.26, 924.14 and 579.74cm^{-1}. The broader stretch at 3285.18cm^{-1} and 2928.75cm^{-1} indicated the presence of -O-H functional group which represents the presence of alcohol and/or free water. The absorption band at 1046.01 cm^{-1} represents the -C-N functional group of aromatic amines, 989.26cm^{-1} showed the functional group, =C-H, of alkenes, 924.14cm^{-1} confirmed the presence of -[C=O-O-H] which is the functional group of carboxylic acid and 579.74 cm^{-1} indicated the -N-H bend of amines in this FT-IR spectra of the boiled plant extract.

The absorption bands at 989.26cm^{-1} and 1228.69cm^{-1} disappeared representing alkenes and aliphatic amines respectively when FT-IR spectrum of the AuNPs was compared with pure boiled plant extract. The disappearance of these two peaks suggested that the =C-H and -C-N, functional group containing compounds might be responsible for the reduction of Au^{++} of $AuCl_3$ to AuNPs. The alkenes can be reduced to alkanes in the presence of metal catalyst like Au, Ag or Pt during the process and the Au^{++} may be reduced to form nano-particles. Aliphatic amines which have no aromatic ring directly attached to the nitrogen atom and also have a lone pair of electrons might be responsible for the reduction of Au^{++} to AuNPs. Comparative FT-IR spectrum of pure boiled plant extract and the synthesized AuNPs further suggested that there was a small change of wave numbers in other absorptions bands. Comparison of the two spectra indicated the shift of the wave numbers at the larger stretch which confers that a small amount of these functional group containing compounds might be involved in the synthesis of AuNPs (Jayaseelan *et al*., 2013).

XRD analysis reveals the size and nature of the crystallite (Sarvesh *et al*., 2013). The two theta (2θ) valves of a number of Bragg's reflections were 38.03°, 46.18° and 63.43° which corresponds to (111), (200) and (220) facets of AuNPs showing the bands for face centered cubic structures of Au. Our results are in complete agreement with Jayaseelan *et al*. (2013) and Nagaraj *et al*. (2014) who reported the same Bragg's reflections. The XRD pattern of the freeze dried sample of AuNPs thus clearly indicated the synthesis of crystalline AuNPs (Harekrishna *et al*., 2009). The average size of AuNPs revealed that the nano-crystallite size of AuNPs was 6.99nm which is in

agreement with AFM data (Nagaraj *et al*., 2014). The sharpness of the first peak clearly showed that the synthesized AuNPs were in nano region. There were no peaks for the XRD patterns due to the crystallographic impurities showing the AuNPs synthesized were highly in pure form (Pathipati and Rajasekharreddy, 2011).

MALDI-TOF is a method of mass spectroscopy in which the mass to charge ratio of an ion is determined through the measurement of the time of flight of the ion. The ion is accelerated in an electric field of known high strength. This acceleration produces ions with same kinetic energy. The velocity of the ion depends on the mass to charge ratio. The time that is subsequently taken by the particle to reach the detector present at a known distance. Heavier particles will take longer while lighter particles will take shorter time to reach the detector and from this phenomenon the charge to mass ratio of the ion is calculated (Ateeq *et al*., 2015). In the present study, we used MALDI-TOF technique for the first time to formulate structure for the AuNPs synthesized from plant extract. The data obtained from MALDI-TOF analysis indicated that one gold molecule was lost during fragmentation. Atomic weight of Au is 196.97amu and Cl is 35.5amu. The difference among all the peaks is almost 197, which indicated that only one gold molecule was fragmented during the process. As the extract contained a large number of molecules and we do not know the exact moment about the fragmentation of the molecule, therefore, the contribution from the extract was designated as 'L_x', the contribution from the Chloride as 'Cl_y' and the gold atom which is lost during fragmentation is shown as Au_x. the possible formulated structure was $[Au_xL_xCl_y]^{x+}$. It can be deduced from the spectrogram that the fragmentation of Au and extract occurred with 1:1 ratio showing that the nano-particles lost one gold atom during fragmentation while the ligand was intact.

AFM unlike other microscopic techniques offer three dimensional visualization. The AFM analysis clearly confirmed that different sizes of AuNPs were synthesized. The diameter of the smallest nano-particles was found to be 1.5nm while the largest nanoparticle was 6.5nm. These results are in complete agreement with XRD data, where the size of crystallite was calculated to be 6.99 nm. Different sizes (2-7nm) of nanoparticles were synthesized in different percentages. In the present study antibacterial activity of AuNPs was also carried out against seven strains. The AuNPs were active against all the bacterial strains used and the activity was dose dependent. Maximum growth reduction was shown by AuNPs at highest concentration against *E. coli* while minimum growth reduction was noted at lowest concentration against *P. aeruginosa* and *C. freundii*. *K. pnemoniae, E. coli* and *X. compestris* exhibited high degree of sensitivity, *B. subtilis* and *C. freundii* moderate while *P. aeroginosa*, *S. aureus and C. freundii* exhibited least sensitivity to AuNPs. The AuNPs enhanced the activity of the extract against the tested bacteria. Similar results are also reported by Ameer *et al*. (2009), Me´ndez *et al*. (2011), Prasad *et al*. (2011), Sarvesh *et al*. (2013), Malarkodi *et al*. (2013), Logeswari *et al*. (2013), Nagaraj *et al*. (2014) and Kumar *et al*. (2011).

The antifungal activity of AuNPs of *Periploca hydaspidis* was also carried out against *C. albicans* and *P. chrysogynum*. The results suggested that *C. albicans* was responsive to AuNPs at all concentrations used. Maximum growth inhibition was demonstrated by AuNPs at highest concentrations and minimum at 300 against both fungi. Our results agree with Jayaseelan *et al*. (2013) who concluded that all the fungal strains were susceptible to the AuNPs. All the other strains used during the present study were completely resistant to the AuNPs showing no zone of inhibition at all the tested concentrations.

Plants produce compounds which possesses the ability to scavenge free radicals. These biomoelcules include phenolic acids, lignins, tannins, alkaloids, terpenoids, flavonoids, stilbenes, coumarins, amines and vitamins etc. (Cai*et al*., 2003). These compounds possess anti-inflammatory, antimutagenic, antibacterial, antiviral, antiatherosclerotic, antitumor, and anticarcinogenic, capabilities (Sala *et al*., 2002). These compounds can reduce the risk of happening of cancer, heart disease, diabetes, and other complications when taken as natural antioxidants through diet or through medicine prepared from plants (Veerapur *et al*., 2009). Besides, the projected life of food and food goods can be improved by accretion of antioxidants (Cook and Samman, 1996). DPPH free radical scavenging assay revealed dose dependent antioxidant activity. Increasing concentration of the AuNPs increased antioxidant at highest concentration of the AuNPs.

ACKNOWLEDGMENTS

The authors acknowledge the financial support of Higher Education Commission Islamabad Pakistan.

CONCLUSION

It can be concluded from these results that AuNPs were more stable at 1mM concentration of the salt, neutral to slightly basic pH and temperature from 24°C to 39°C,. Alkenes and aliphatic amines were responsible for the formation of AuNPs. The nanocrystallite size was 6.99nm and cubic in nature. The synthesized nano-particles revealed good anti-oxidant and anti-microbial activities.

REFERENCES

Amarendra DD and Gopal K. (2010). Biosynthesis of silver and gold nanoparticles using *Chenopodium*

album leaf extracts. *Colloids and Surf. A: Physicochem Engg Aspects.,* **369**: 2733.

Ameer A, Ahmed F, Arshi N, Chaman M and Naqvi AH (2009). One step synthesis and characterization of gold nanoparticles and their antibacterial activities against *E. coli* (ATCC 25922 strain). *Intl. J. Theor. Appl. Sci.,* **1**: 1-4.

Ashok B, Joshi B, Kumar AR and Zinjarde S (2010). Banana peel extract mediated novel route for the synthesis of silver nanoparticles. *Colloids and Surf. A: Physicochem Engg. Aspects.*, **368**: 58-63.

Ateeq M, Shah MR, Ain N, Bano S, Anis I, Lubna Faizi S, Bertino MF and Naz SS (2015). Green synthesis and molecular recognition ability of patuletin coated gold nanoparticles. *Biosen. Bioelectr.,* **63**: 499-505.

Bakht J, Zainab I, Shafi M and Arshad I (2017). Screening of medicinally important *Berberis lyceum* for their antimicrobial activity by disc diffusion assay. *Pak. J. Pharmaceut. Sci*., **30**: 1783-1789.

Bauer AW, Kirby WMM, Sherris JC and Turck M (1966). Antibiotic susceptibility testing by standardized single disk method. *Am. J. Clin. Pathol.,* **45**: 493-496.

Cait YZ, Sun M and Corke H (2003). Antioxidant activity of betalains from plants of the *Amaranthaceae***.** *J. Agric. Food Chem.*, **51**: 2288-2294.

Chandran SP, Chaudhary P, Pasricha R, Ahmad A and Sastry M (2006). Synthesis of gold Nanotriangles and silver nanoparticles using *Aloe vera* plant extract. *Biotechnol. Prog*., **22**:77-583.

Cook NC and Samman S (1996). Flavonoids-chemistry, metabolism, cardioprotective effect and dietary sources. *The J. Nutr. Biochem.*, **7**: 66-76.

Dubey SP, Dwivedi AD, Lahtinen M, Lee C, Kwon Y and Sillanpaa M (2013). Protocol for development of various plants leaves extract in single-pot synthesis of metal nanoparticles. *Spectrochimica Acta Part A: Molecu. Biomolec. Spectro*., **103**: 134-142.

Genc R, Clergeaud G, Ortiz M and O'Sullivan CK (2011). Green synthesis of gold nanoparticles using glycerol-incorporated nanosized liposomes. Langmuir., **27**: 10894-10900.

Gnanajobitha G, Vanaja M, Paulkumar K, Rajeshkumar S, Malarkodi C, Annadurai G and Kannan C (2013). Green synthesis of silver nanoparticles using *Millingtonia hortensis* and evaluation of their antimicrobial efficacy. *Intl. J. Nanomat. Biostruct*., **3**: 21-25.

Harekrishna B, Bhui KD, Gobinda P, Sahoo P, Sarkar P and Ajay D (2009). Green synthesis of Silver nanoparticles using latex of *Jatropha curcas. Colloids and Surf A: Phytochem. Engg. Aspect.,* **339**: 134-139.

Haung X, Prashant KJ, Ivan HE and Mostafa AE (2007). Gold nanoparticles: Interesting optical and recent application in cancer diagnostics and theraphy. *Nanomed*., **2**: 881-693.

Jayaseelan C, Ramkumar R, Rahuman A and Perumal P. (2013). Green synthesis of gold nanoparticles using seed aqueous extract of *Abelmoschus esculentus* and its antifungal activity. *Indust. Crops Prod*., **45**: 423-429.

Krishnaraj C, Ramachandran R, Mohan K and Kalaichelvan PT (2012). Optimization for rapid synthesis of silver nanoparticles and its effect on phytopathogenic fungi. *Spectrochimica Acta Part A: Molecu. Biomolec. Spectro.,* **93**: 95-99.

Kumar GV, Gokavarapub SD, Rajeswarib A, Dhasa TS, Karthicka V, Kapadiab Z, Shresthab T, Barathyb IA, Royb A and Sinhab S (2011). Facile green synthesis of gold nanoparticles using leaf extract of antidiabetic potent *Cassia auriculata. Colloids and Surf. B: Biointer.,* **87**: 159-163.

Lim CK, Heo J, Shin S, Jeong K and Seo YH (2013). Nanophotosensitizers toward advanced Photodynamic therapy of Cancer. *Cancer Lett*., **334**: 176-187.

Logeswari P, Silambarasan S and Abraham J (2013). Ecofriendly synthesis of silver nanoparticles from commercially available plant powders and their antibacterial properties. *Scientia Iranica.*, **3**:1049-1054.

Malarkodi C, Rajeshkumar S, Vanaja M, Paulkumar K, Gnanajobitha G and Annadurai G (2013).Eco-friendly synthesis and characterization of gold nanoparticles using *Klebsiella pneumoniae*. *J. Nanostruct. Chem.,* **3**: 30-37.

Mann S (1996). Biomimetic Materials Chemistry. VCH, New York.

Me´ndez MAA, Martı´n-Martı´nez ES, Ortega-Arroyo L, Portillo GC and S.Espı´ndola E (2011). Synthesis and characterization of silver nanoparticles: Effect on phytopathogen Colletotrichum gloesporioides. *J. Nanopart. Res.,* **13**: 2525-2532.

Mensor LI, Menezes FS and Leitao GG (2001). Screening of Brazillian plant extracts for antioxidant activity by the use of DPPH free radical method. *Phytother. Res.*, **15**: 127-130.

Nagaraj B, Idhayadhulla A and Lee YR (2014). Industrial crops and products phyto-synthesis of gold nanoparticles using fruit extract of *Hovenia dulcis* and their biological activities. *Indust. Crops Prod.,* **52**: 745-751.

Nasir A, Dawood A and Bakht J (2015). Antibacterial activity of different solvent extracted samples from the flowers of medicinally important *Plumeria obstusa*. *Pak. J. Pharmaceut. Sci.,* **28**: 195-2000.

Noruzi M, Zare D, Khoshnevisan K and Davoodi D (2011). Rapid green synthesis of gold Nanoparticles using *Rosa hybrida* petal extract at room temperature. *Spectrochimica Acta Part A: Molecu. Biomolec. Spectro*., **79**: 1461-1465.

Ocanas LG, Ferrer DA, Burt J, Torres LAD, Cabrera MR, Rodriguez VT, Rangel RL, Romanovicz R and Yacaman MJ (2010). Biodistribution and long-term fate of silver nanoparticles functionalized with bovine serum albumin in rats. *Metallomics*, **2**: 204-210.

Pathipati UR and Rajasekharreddy P (2011). Green synthesis of silver-protein (core-shell) nanoparticles

using *Piper betle* L. leaf extract and its ecotoxicological studies on *Daphnia magna. Colloids and Surf. A: Physicochem. Engg. Aspects,* **38**: 188-194.

Paulkumar K, Rajeshkumar S, Gnanajobitha G, Vanaja Malarkodi C and Annadurai G (2013). Eco Friendly synthesis of silver chloride nanoparticles using *Klebsiella planticola* (MTCC 2277). *Intl. J. Green Chem. Bioproc*., **3**: 12-16.

Phillips KS, Han JH, Martinez M, Wang ZZ, Carter D and Cheng Q (2006). Nanoscale classification of gold substrates for surface plasmon resonance analysis of protein toxins with supported lipid membranes. *Ann. Chem*., **78**: 596-603.

Prasad TNVKV, Elumalai EK and Khateeja S (2011). Evaluation of the antimicrobial efficacy of phytogenic silver nanoparticles. *Asian Pacif. J. Trop. Biomed.,* **1**: 82-85.

Prime KL and Whitesides GM (1991). Self-assembled organic monolayers: model systems for studying adsorption of proteins at surfaces. *Sci.,* **252**: 1164-1167.

Raghavan V, Connolly JM, Fan HM, Dockery P and Wheatley A (2014). Gold nanosensitisers for multimodal optical diagnostic imaging and therapy of Cancer. *J. Nanomed. Nanotechnol*., **5**: 238-148.

Ravichandran V, Tiah ZX, Subashini G, Terence FWX, Eddy FCY, Nelson J and Sokkalingam AD (2011). Biosynthesis of silver nanoparticles using mangos teen leaf extract and evaluation of Their antimicrobial activities. *J. Saudi Chem. Soc*., **15**: 113-120.

Ravindran A, Singh A, Raichur AM, Chandrasekaran N and Mukherjee A (2010). Studies on interaction of colloidal Ag nanoparticles with bovine serum albumin (BSA). *Colloids and Surf. B: Biointer*., **76**: 32-37.

Russel DF and Eisensmith SP (1983). MSTAT-C. Crop Soil Science Department, Michigan State University USA.

Sala A, Recio MD, Giner RM, Manez S, Tournier H, Schinella G and Rios JL (2002). Anti Inflammatory and antioxidant properties of *Helichrysum italicum*. *J. Pharma. Pharmacol*., **54**: 365-371.

Sarvesh KS, Yamada R, Ogino C and Kondo A (2013). Biogenic synthesis and characterization of Gold nanoparticles by *Escherichia coli* K12 and its heterogeneous catalysis in degradation of 4 nitrophenol. *Nanoscale Res. Lett*., **8**: 70-79.

Shankar SS, Ahmad A, Pasrichaa R and Sastry M (2003). Bioreduction of chloroaurate ions by Geranium leaves and its endophytic fungus yields gold nanoparticles of different shapes. *J. Mat.Chem*., **13**: 1822-1826.

Song JY and Kim BS (2009). Rapid biological synthesis of silver nanoparticles using plant leaf extracts. *Bioproc. Biosyst. Engg.*, **32**: 79-84.

Steel RGD, Torrie JH and Dickey DA (1997). Principles and procedures of statistics. *A Biometrical Approach*, 3rd Ed. pp: 172-177. McGraw Hill Book Co. Inc. New York USA.

Valentina AL and Minaev BF (2014). The size-controllable, one-step synthesis and characterization of gold nanoparticles protected by synthetic humic substances. *Mat. Chem. Phys.,* **30**: 1-11.

Veerapur VP, Prabhakar KR and Parihar VP (2009). *Ficus racemosa* stem bark extract: A potent antioxidant and a probable natural radioprotector. *Evid. Based Complem. Alterna. Med.,* **6**: 317-324.

Wajid A, Bakht J and Bilal M (2017). *In vitro* antifungal, antioxidant and HPLC analysis of the extracts of *Physalis philadelphica. Bangladesh J. Pharmacol*., **12**: 313-318.